PAPER

Cinchona alkaloids – acid, anion-driven fluorescent INHIBIT logic gates with a receptor1–fluorophore–spacer–receptor2 format and PET and ICT mechanisms

Nicola' Agius [ID] and David C. Magri [ID] *

The fluorescent natural products, quinine, quinidine, cinchonine and cinchonidine are demonstrated as H^+-enabled, halide-disabled (Cl^-, Br^- or I^-) INHIBIT and INHIBIT-OR combinatorial logic gates in water. More fluorescent natural products with intrinsic logic properties await to be discovered.

Introduction

Fluorescent natural products are wonderous compounds.[1] Many have potent cancer inhibition properties, and meet the standards for use as clinical chemotherapeutic agents.[2] Other fluorescent natural products, such as photofrin and hypericin, are used in photodynamic therapy.[3] The natural product, quinine (Fig. 1), was the first drug treatment for malaria, and remains the key ingredient of tonic water, and a primary fluorescence quantum yield standard ($\Phi_F = 0.55$ in H_2SO_4 0.1 M).[4] Its diastereomeric sister molecule, quinidine (Fig. 1), is used as an antiarrhythmic agent for the treatment of heart conditions.[5] These *cinchona* alkaloids have five stereocenters, the same 1S, 3R, 4S stereochemistry at the bicyclic bridgehead nitrogen and carbon stereocenters, and opposite stereochemistry at the 8 and 9 carbon atoms (*i.e.* quinidine 8R and 9S).[6] There are other noteworthy structural features, including a 6-methoxyquinoline fluorophore, an azabicyclic amine and a vinyl moiety. The synthesis of quinine and quinidine in the organic chemistry lab is a classic fable of serendipity, controversy and hard work.[7–9] Their cousins, cinchonine and cinchonidine (Fig. 1), are nearly identical, except that the quinoline fluorophore lacks the 6-methoxy moiety.[10]

The connectivity of these structural features is truly remarkable. Nature has conveniently engineered the *cinchona* alkaloids in a modular fashion consistent with the design principles of photoinduced electron transfer (PET)[11] and photoinduced internal charge transfer (ICT).[12] All four molecules, **1–4** have a hybrid receptor1–fluorophore–spacer–receptor2 arrangement (Fig. 1).[13,14] Receptor1 is the nitrogen atom within quinoline and receptor2 is the azabicyclic amine. The spacer is the hydroxylated ethylene unit and the fluorophore is the 6-methoxyquinoline or quinoline moiety. This architecture is a fusion of the fluorophore–receptor ICT sensors popularised by Valeur[15] and the fluorophore–spacer–receptor PET sensors/switches popularised by de Silva.[16] The molecular engineering aspects of quinine and cinchonidine were hinted as fluorescent indicators during the infancy of PET; however, the hybrid design format and their function as logic gates was overlooked.[17]

The first hybrid PET-ICT logic gates were reported two decades ago.[18] Pérez-Inestrosa described reconfigurable logic gates based on a benzylisoquinoline *N*-oxide appended with benzo-15-crown-5 ether or methoxyphenol.[13] We have demonstrated this hybrid design concept using lab synthesised 1,3,5-triaryl-Δ^2-pyrazolines as H^+-driven off–on–off ternary logic gates.[14] Now we demonstrate that the *cinchona* alkaloids are receptor1–fluorophore–spacer–receptor2 fluorescent logic gates. Being commercially available,[19] there was no need for synthetic effort.

In this study, we present the natural products, quinidine **1**, quinine **2**, cinchonine **3** and cinchonidine **4** as combinatorial fluorescent molecular logic gates.[20,21] We demonstrate that all four molecules are examples of H^+, Cl^--driven INHIBIT[22] logic
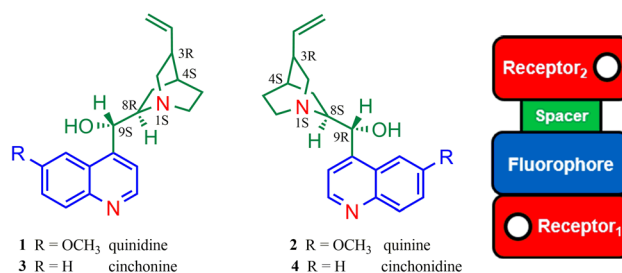
Department of Chemistry, Faculty of Science, University of Malta, Msida, MSD 2080, Malta. E-mail: david.magri@um.edu.mt

Fig. 1 The *cinchona* alkaloids quinidine **1**, quinine **2**, cinchonine **3** and cinchonidine **4** and the colour-coded modular hybrid design inclusive of photoinduced electron transfer (PET) and internal charge transfer (ICT).

gates in water with H^+ as the enabling input, and Cl^- as the disabling input.[23] The logic application can be extended to other anions such as Br^- and I^-, which introduces an additional OR function. Chloride and iodide have physiological significance, while bromide is considered a non-essential trace element.[24] A high level of chloride in bodily fluids is a diagnostic parameter for cystic fibrosis.[25] Patients of this illness have elevated Cl^- levels in sweat and saliva.[26] Bromide and iodide are diagnostic for hematologic and thyroid diseases.[27]

Results & discussion

Spectroscopic results

The UV-visible absorption spectra of **1–4** were studied in water (Table 1, Fig. 2). At basic pH, the λ_{abs} of the 6-methoxyquinoline within **1** and **2** is observed at 328 nm and the λ_{abs} of quinoline within **3** and **4** is observed at the shorter wavelengths of 274 nm and 272 nm. At acidic pH, the λ_{abs} is red-shifted 22 nm for **1** and **2**, and 40 nm for **3** and **4**. The molar extinction coefficients in logarithm form ($\log \varepsilon$) are intense ranging from 3.3 in base to 4.1 in acid. The difference in the peak maxima between **1** and **2** versus **3** and **4** is attributed to the electron-donating methoxy group. Isosbestic points are observed at 263 nm, 300 nm and 334 nm for **1**, and at 298 nm and 306 nm for **2**. Isosbestic points are also observed for **3** at 258 nm and 306 nm, and for **4** at 252 nm, 282 nm and 297 nm. These observations for **1** and **2** are in good agreement with literature results.[28]

The emission properties of **1–4** in water are provided in the lower half of Table 1 and the emission spectra are shown in Fig. 3. In protic solvents, including water, the emission is bright due to a π, π^* transition (while in non-polar solvent there is an inversion to a n, π^* state).[4] At basic conditions of 10^{-11} M H^+, the emission is weak with the λ_{max} situated at 385 nm. At 10^{-6} M H^+, the azabicyclic amine is protonated resulting in a modest fluorescence increase. Both **1** and **2** emit a bright, blue fluorescence with 10^{-2} M H^+.[23] The emission spectra are broad with maxima at 450 nm and 448 nm. On titration with acid, an
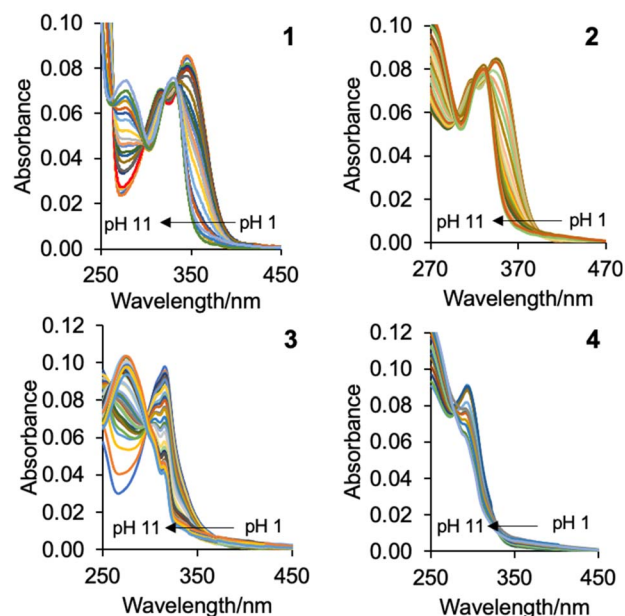

Fig. 2 The UV-vis absorption spectra of **1–4** in water excited at 350 nm, 350 nm, 312 nm and 315 nm, respectively, as a function of pH.

isoemissive point is observed at 394 nm and 400 nm for **1** and **2**, respectively. In contrast, the peak maxima of **3** and **4** are observed at 431 nm and 412 nm, and isoemissive points appear at 371 nm and 350 nm.

The excited state $pK_a s^*$ were evaluated by titrating **1–4** with aliquots of acid and fitting the intensity-pH data to the Henderson–Hasselbalch equation derived for spectrofluorimetric analysis (see footnote in Table 1). Two $pK_a s^*$ are clearly evident
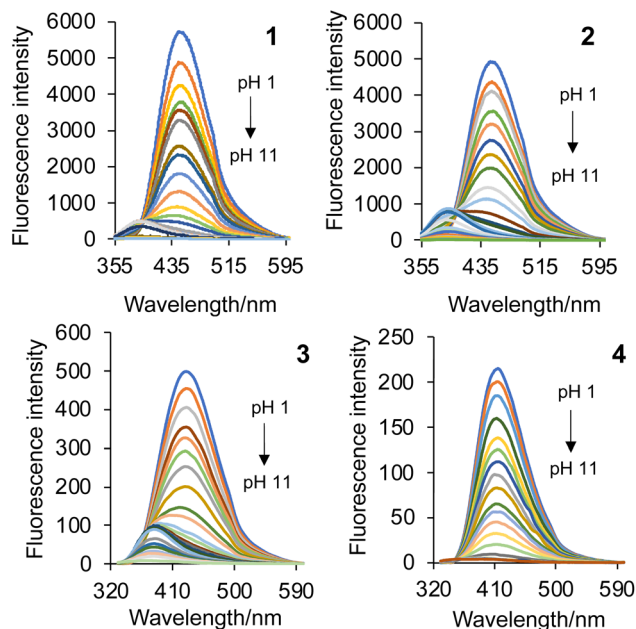
Table 1 Photophysical properties of **1–4** in water[a]

	1	**2**	**3**	**4**
$\lambda_{Abs\ pH\ 11}/nm$[b]	328	328	274	272
$\log \varepsilon_{pH\ 11}$	3.37	3.32	3.33	3.38
$\lambda_{Abs\ pH\ 2}/nm$[c]	350	350	315	312
$\log \varepsilon_{pH\ 2}$	4.08	3.74	3.92	3.84
$\lambda_{Abs(isos)}/nm$	263, 300, 334	298, 306	258, 306	252, 282, 297
$\lambda_{Flu\ pH\ 11}/nm$	385	386	383	400
$\lambda_{Flu\ pH\ 2}/nm$	450	448	431	412
$\lambda_{Flu(isos)}/nm$	394	400	371	350
pK_a^{*}[d]	4.40, 9.05	4.20, 9.20	4.10, 9.00	4.10[f]
FE[e]	186	197	116	48

[a] 184 μM **1**, 548 μM **2**, 2.0 mM **3**, 2.2 mM **4**. In presence of 1 μM Na_2EDTA. [b] Basic pH adjusted with 0.10 M $(CH_3)_4NOH$. [c] Acidic pH adjusted with 0.10 M CH_3SO_3H. [d] Excited state pK_as determined by $\log[(I_{max} - I)/(I - I_{min})] = -\log[H^+] + \log \beta_{H^+}$ from emission spectra in water buffered with 0.1 μM Na_2EDTA. Emission spectra obtained by excitation at λ_{Isos}. [e] H^+-induced fluorescence enhancement (FE) $I_{FpH\ 2}/I_{FpH\ 11}$. [f] Only one inflection point is observed from I-pH plot.

Fig. 3 The emission spectra of **1–4** in water excited at 350 nm, 350 nm, 312 nm and 315 nm, respectively, as a function of pH.

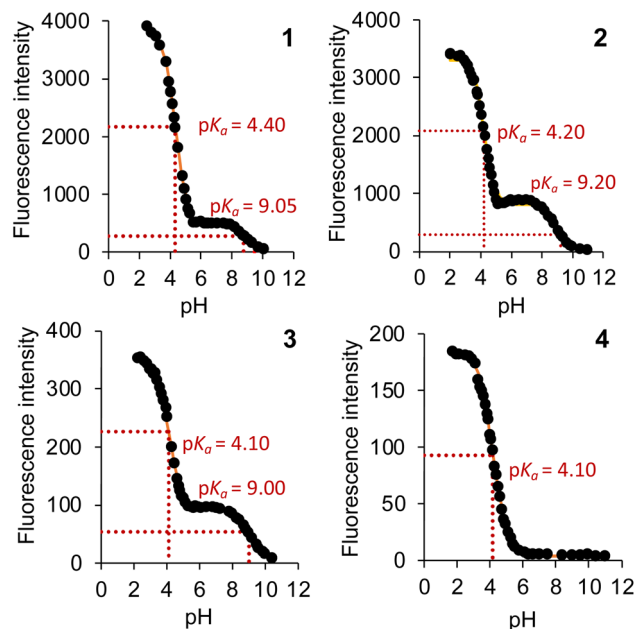**Fig. 4** Maximum peak intensity-pH plots of **1–4** in water labelled with the excited state pK_as.

Fig. 5 The emission spectra of **1–4** in water illustrating the four H$^+$, Cl$^-$-driven INHIBIT logic scenarios. The numbers in parentheses are the binary input conditions in Table 2.

for **1–3** in a stepwise manner at *ca.* 9.00 and 4.20 (Fig. 4), which are attributed to protonation of the azabicyclic and quinoline nitrogen atoms, respectively.[26] Compound **3** similarly has pK_as* at 4.10 and 9.00, while diastereomer **4** has only a single pK_a^* of 4.10 (Fig. 4). The greatest fluorescence enhancement (FE) occurs upon the second protonation as shown in Fig. 4. Alkaloids **1** and **2** exhibit excellent FE ratios of 186 and 197-fold ($I_{FpH\ 2}/I_{FpH\ 11}$). Similar characteristics are observed with **3** and **4**, but with the absence of the methoxy group, the charge transfer character is not as dominant. The FEs of **3** and **4** are a respectable 116 and 48-fold.

Molecular logic

The *cinchona* alkaloids **1–4** function as H$^+$, Cl$^-$-driven INHIBIT logic gates.[22,23] The truth tables for the four input scenarios are summarised in Table 2 and the corresponding emission spectra are provided in Fig. 5. H$^+$ and Cl$^-$ are the inputs and emission is the output. At 10^{-6} M H$^+$, the emission of the monoprotonated state is partially turned on due to protonation of the azabicyclic amine, which prevents photoinduced electron transfer to the
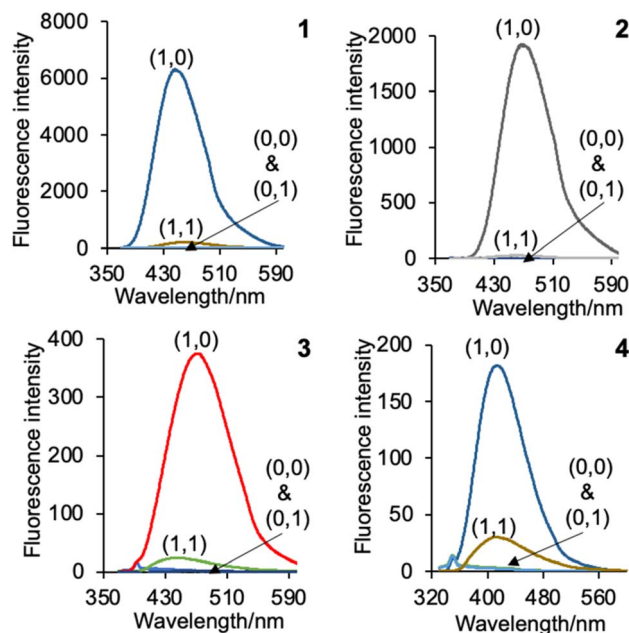
fluorophore. At a higher concentration of 10^{-2} M H$^+$, protonation also occurs at the quinoline nitrogen atom. The fluorescence quantum yields (Φ_F) of **1** and **2** in the dication state are 0.55 and 0.52.[28] The maximum Φ_Fs of **3** and **4** are an order of magnitude lower at 0.052 and 0.022. The off states of **1–4** are all below naked eye detection on irradiation of solutions with a 365 nm UV lamp. Visible discrimination between the on state (blue emission) and the three off states (colourless) is digitally visible for **1–3**. The on state of **4** is too weak to be deciphered with the naked eye. All of the molecules are non-fluorescent in the absence of H$^+$ and Cl$^-$, in the presence of Cl$^-$, and in the presence of both H$^+$ and Cl$^-$. A high emission results only at highly acidic conditions when **1–4** are charged dication species in the absence of Cl$^-$.[27]

High levels of Cl$^-$, Br$^-$ or I$^-$ in the absence, as well as in the presence, of acid turn off the emission of **1–4** by collisional quenching, which results in deactivation of the singlet excited state.[29] The dynamic quenching of the halides follows the order I$^-$ > Br$^-$ > Cl$^-$. While 1 mM of I$^-$ was sufficient for complete quenching of the emission for all four compounds, 1 mM of

Table 2 Truth tables for INHIBIT logic gates **1–4** with H$^+$ and Cl$^-$ in water[a,b]

Input$_1$ (H$^+$)[c]	Input$_2$ (Cl$^-$)[d]	Output **1** (Φ_F)[e]	Output **2** (Φ_F)[e]	Output **3** (Φ_F)[e]	Output **4** (Φ_F)[e]
0 (low)	0 (low)	0 (0.002)	0 (0.003)	0 (0.001)	0 (0.001)
1 (high)	0 (low)	1 (0.553)	1 (0.523)	1 (0.052)	1 (0.022)
0 (low)	1 (high)	0 (0.002)	0 (0.003)	0 (0.001)	0 (0.001)
1 (high)	1 (high)	0 (0.003)	0 (0.003)	0 (0.002)	0 (0.002)

[a] 0.184 mM **1**, 0.548 mM **2**, 2.0 mM **3**, 2.2 mM **4**. In presence of 0.1 μM Na$_2$EDTA. [b] Excited at 350 nm, 350 nm, 315 nm, and 312 nm. [c] High input$_1$ 10^{-2} M H$^+$ and low input$_1$ H$^+$ 10^{-11} M adjusted with CH$_3$SO$_3$H and (CH$_3$)$_4$NOH. [d] High input$_2$ 100 mM Cl$^-$ and low input$_2$ no Cl$^-$ added as NaCl. [e] Relative Φ_F of **1** and **2** *versus* 10^{-6} M quinine sulfate in aerated 0.1 M H$_2$SO (Φ_F = 0.55). High threshold output level set at $\Phi_{Fmax}/2$.

Table 3 Partial truth table entries for OR-INHIBIT logic and fluorescence quantum yields of **1–4** with H$^+$ and Br$^-$ or I$^-$ in water[a,b]

Input$_1$ (H$^+$)[c]	Input$_2$ (Br$^-$ or I$^-$)[d]	Output 1 (Φ_F)[e]	Output 2 (Φ_F)[e]	Output 3 (Φ_F)[e]	Output 4 (Φ_F)[e]
0 (low)	1 (1 mM Br$^-$, high)	0 (0.009)	0 (0.023)	0 (0.002)	0 (0.001)
0 (low)	1 (100 mM Br$^-$, high)	0 (0.002)	0 (0.002)	0 (0.001)	0 (0.001)
1 (high)	1 (1 mM Br$^-$, high)	0 (0.042)	0 (0.036)	0 (0.009)	0 (0.005)
1 (high)	1 (100 mM Br$^-$, high)	0 (0.002)	0 (0.002)	0 (0.001)	0 (0.001)
0 (low)	1 (1 mM I$^-$, high)	0 (0.001)	0 (0.007)	0 (0.001)	0 (0.001)
1 (high)	1 (1 mM I$^-$, high)	0 (0.001)	0 (0.001)	0 (0.001)	0 (0.001)

[a] 0.184 mM **1**, 0.548 mM **2**, 2.0 mM **3**, 2.2 mM **4**. [b] Excited at 350 nm, 350 nm, 315 nm and 312 nm. [c] High input$_1$ 10^{-2} M H$^+$ and low input$_1$ H$^+$ 10^{-11} M adjusted with CH$_3$SO$_3$H and (CH$_3$)$_4$NOH. [d] High input$_2$ 1 mM or 100 mM for Br$^-$, or 1 mM for I$^-$. [e] Relative Φ_F of **1** and **2** versus 10^{-6} M quinine sulfate in aerated 0.1 M H$_2$SO ($\Phi_f = 0.55$).

Br$^-$ was not adequate for quenching the emission of **1** and **2** in the presence of 10^{-2} M H$^+$ (Table 3). However, the addition of 100 mM Cl$^-$ (Table 2) or 100 mM Br$^-$ (Table 3) sufficiently quenches the emission. The trend is due to the efficiency of intersystem crossing to the excited triplet state, promoted by spin–orbit coupling between the excited singlet fluorophore and the halide due to the heavy-atom effect.[30] In all cases, aliquots of halide cause the fluorescence intensity to decrease linearly according to the Stern–Volmer equation.[26]

Hence, the necessity for selecting an appropriate acid when conducting fluorescence analyses, for example, of quinine content in urine or tonic water.[31,32] From a practical point of view, it has been known for over a century that hydrochloric acid, and other halide acids, are not suitable reagents for analytical fluorescence studies.[31] We selected methanesulfonic acid in order to minimise fluorescence quenching by the counterion.[32,33] The convention is to use an oxyacid, such as sulfuric acid, to acidify a quinine solution for Φ_F measurements.[4] There are reports of quinolium-based turn off sensors for halides,[34] however, they were not examined from a Boolean perspective. A notable exception is the recent development of contact lens for measuring sodium Na$^+$ and Cl$^-$ ions in tears.[35] The adaptation of fluorescent dye-appended azacryptands as turn-on probes for anions nicely illustrates further opportunities for the development of H$^+$, anion-driven logic gates for selective acid-anion detection.[36]

Conclusions

In summary, the *cinchona* alkaloids are demonstrated as H$^+$, Cl$^-$-driven INHIBIT logic gates with Cl$^-$ as the disabling input. Consideration of other heavier halides such as Br$^-$ and I$^-$ as disabling inputs expands the operation to a combinatorial OR-INHIBIT logic gate. The logic functions of the *cinchona* alkaloids, could in principle, be expanded by incorporating a third receptor (or electron donor)[37] by covalent attachment of a receptor to the alcohol or vinyl moieties resulting in a three-input logic gate.[38] In fact, derivatization of the natural product, anabasine, yielded the first molecular logic gate with three PET processes and three cation binding sites as an off–on–off Na$^+$-enable proton switch.[39] A coumarin-anabasine conjugate exemplifies an off–on–off H$^+$-enabled ternary logic gate[40] as does a dihydroxylated nigakinone.[41] Although not explicitly

mentioned earlier, a H$^+$-driven 'low-medium-high' emission profile is observable in Fig. 4 for the *cinchona* alkaloids **1–3**.[18]

Creativity in chemistry is often perceived as the design and creation of new reactions and molecules. The field of molecular-logic based computation came to fruition in 1993 with the demonstration of a synthetic fluorescent AND logic gate.[17b] The first INHIBIT logic gate, seven years later, was also a synthetic creation.[22] Creativity, though, may also arise from novel conceptual interpretations of well-known chemical reactions or well-established molecules, elegantly stated in the adage, "old molecules, new concepts".[42] Fluorescein was demonstrated as a moleculator;[43] the metal complex, tris(bipyridine)ruthenium(II) chloride as a 4-to-2 encoder and 2-to-4 decoder;[42] and a dithienylethene photochrome as a set-reset latch.[44] The *cinchona* alkaloids, isolated in the 1820s, have been readily available as INIHIBIT fluorescent logic gates, like diamonds in the Earth, waiting to be discovered. We envision that the screening of fluorescent natural products from a molecular logic viewpoint should result in the discovery of other Nature-derived fluorescent switches and logic gates.

Author contributions

Conceptualization (DCM), investigation (NA), methodology (DCM), visualization (NA, DCM), supervision (DCM) and writing (DCM).

Conflicts of interest

There are no conflicts of interest to declare.

Acknowledgements

Notes and references

1 H. Yuan, A. Jiang, H. Fang, Y. Chen and Z. Guo, *Adv. Drug Delivery Rev.*, 2021, **179**, 113917.
2 R. Duval and C. Duplais, *Nat. Prod. Rep.*, 2017, **34**, 161.
3 B. Mansoori, A. Mohammadi, M. Amin Doustvandi, F. Mohammadnejad, F. Kamari, M. F. Gjerstorff,

B. Baradaran and M. R. Hamblin, *Photodiagn. Photodyn. Ther.*, 2019, **26**, 395.

4 B. Valeur and M. N. Berberan-Santos, *Molecular Fluorescence: Principles and Applications*, John Wiley & Sons, Weinheim, 2012.

5 S. L. Rawe and C. McDonnell, The cinchona alkaloids and the aminoquinolines, in *Antimalarial Agents Design and Mechanism of Action*, Elsevier, 2020, ch. 3, p. 65.

6 K. M. Kacprzak, Chemistry and Biology of Cinchona Alkaloids, in *Natural Products*, ed. K. G. Ramawat and J. M. Mérillon, Springer-Verlag Berlin Heidelberg, 2013, ch. 21.

7 I. T. Raheem, S. N. Goodman and E. N. Jacobsen, *J. Am. Chem. Soc.*, 2004, **126**, 706The synthesis has 16 reaction steps.

8 V. Nair, R. S. Menon and S. Vellalath, *Nat. Prod. Commun.*, 2006, **1**, 899The paper gives a historic account of the asymmetric synthesis of quinine.

9 T. Terunuma and Y. Hayashi, *Nat. Commun.*, 2022, **13**, 7503, A five-pot synthesis of (–)-quinine was reported in 14% yield.

10 R. M. Hariyanti, Y. C. Sumirtapura and N. F. Kurniati, *Biointerface Res. Appl. Chem.*, 2023, **13**, 319.

11 (a) A. P. de Silva, H. Q. N. Gunaratne, T. Gunnlaugsson, A. J. M. Huxley, C. P. McCoy, J. T. Rademacher and T. E. Rice, *Chem. Rev.*, 1997, **97**, 1515; (b) J. F. Callan, A. P. de Silva and D. C. Magri, *Tetrahedron*, 2005, **61**, 8551.

12 B. Valeur and I Leray, PCT (Photoinduced Charge Transfer) Fluorescent Molecular Sensors for Cation Recognition in New Trends in Fluorescence Spectroscopy, *Applications to Chemical and Life Sciences*, Springer-Verlag, Berlin, 2001, ch. 10, p. 187.

13 (a) J.-M. Montenegro, E. Pérez-Inestrosa, D. Collado, Y. Vida and R. Suau, *Org. Lett.*, 2004, **6**, 2353; (b) E. Pérez-Inestrosa, J.-M. Montenegro, D. Collado, R. Suau and J. Casado, *J. Phys. Chem. C*, 2007, **111**, 6904.

14 (a) R. Zammit, M. Pappova, E. Zammit, J. Gabarretta and D. C. Magri, *Can. J. Chem.*, 2015, **93**, 199; (b) N. Zerafa, M. Cini and D. C. Magri, *Mol. Syst. Des. Eng.*, 2021, **6**, 93; (c) D. Sammut, N. Bugeja, K. Szaciłowski and D. C. Magri, *New J. Chem.*, 2022, **46**, 1504.

15 B. Valeur and I. Leray, *Coord. Chem. Rev.*, 2000, **205**, 3.

16 (a) J. Ling, B. Daly, V. A. D. Silverson and A. P. de Silva, *Chem. Commun.*, 2015, **51**, 8403; (b) A. J. Bryan, A. P. de Silva, S. A. de Silva, R. A. D. D. Rupasinghe and K. R. A. S. Sandanayake, *Biosensors*, 1989, **4**, 169.

17 (a) R. A. Bissell, E. Calle, A. P. de Silva, S. A de Silva, H. Q. N. Gunaratne, J.-L. Habib-Jiwan, S. L. A. Peiris, R. A. D. D. Rupasinghe, T. K. S. D. Samarasinghe, K. R. A. S. Sandanayake and J.-P. Soumillion, *J. Chem. Soc., Perkin Trans. 2*, 1992, 1559This paper was accepted on the 13th May 1992. The first molecular logic gate was reported on the 1st July 1993.; (b) A. P. Silva, H. Q. N. Gunaratne and C. P. McCoy, *Nature*, 1993, **364**, 42.

18 (a) M. H. Mei and S. K. Wu, *New J. Chem.*, 2001, **25**, 471; (b) J. F. Callan, A. P. de Silva, J. Ferguson, A. J. M. Huxley and A. M. O'Brien, *Tetrahedron*, 2004, **60**, 11125; (c) A. P. de Silva and D. C. Magri, *Chimia*, 2005, **59**, 218.

19 The *cinchona* alkaloids were purchased from TCI Europe with purity >98%. UV-visible absorbance spectra and emission spectra were recorded on Jasco V-650 and FP-9300 spectrophotometers using 1.0 cm Suprasil quartz cuvettes. The spectra were background subtracted for the solvent.

20 (a) C.-Y. Yao, H.-Y. Lin, H. S. N. Cory and A. P. de Silva, *Mol. Syst. Des. Eng.*, 2020, **5**, 1325–1353; (b) D. C. Magri, *Coord. Chem. Rev.*, 2021, **426**, 213598; (c) S. Erbas-Cakmak, T. Gunnlaugsson, S. Kolemen, T. D. James, A. C. Sedgwick, J. Yoon and E. U. Akkaya, *Chem. Soc. Rev.*, 2018, **47**, 2228; (d) J. Andréasson and U. Pischel, *Chem. Soc. Rev.*, 2018, **47**, 2266.

21 A. P. de Silva, *Molecular Logic-based Computation*, The Royal Society of Chemistry, Cambridge, 2013.

22 (a) T. Gunnlaugsson, D. A. Mac Dónail and D. Parker, *Chem. Commun.*, 2000, 93; (b) T. Gunnlaugsson, D. A. Mac Dónail and D. Parker, *J. Am. Chem. Soc.*, 2001, **123**, 12866; (c) M. de Sousa, M. Kluciar, S. Abad, M. A. Miranda, B. de Castro and U. Pischel, *Photochem. Photobiol. Sci.*, 2004, **3**, 639.

23 N. Agius and D. C. Magri, *New J. Chem.*, 2021, **45**, 14360.

24 R. E. Cuenca, W. J. Pories and J. Bray, *Biol. Trace Elem. Res.*, 1988, **16**, 151.

25 (a) C. D. Geddes, *Meas. Sci. Technol.*, 2001, **12**, R53; (b) C. D. Geddes, K. Apperson, J. Karolin and D. J. S. Birch, *Anal. Biochem.*, 2001, **293**, 60; (c) A. C. Gonçalves, F. A. L. Marson, R. M. H. Mendonça, C. S. Bertuzzo, I. A. Paschoal, J. D. Ribeiro, A. F. Ribeiro and C. E. Levy, *J. Pediatr.*, 2019, **95**, 443.

26 D. L. R. Novo, J. E. Mello, F. S. Rondan, A. S. Henn, P. A. Mello and M. F. Mesko, *Talanta*, 2019, **191**, 415.

27 D. Pant, U. C. Tripathi, G. C. Joshi, H. B. Tripathi and D. D. Pant, *J. Photochem. Photobiol., A*, 1990, **51**, 3113.

28 S. G. Schulman, R. M. Threatte, A. C. Capomacchia and W. L. Paul, *J. Pharm. Sci.*, 1974, **63**, 876.

29 N. Kumar Joshi, N. Tewari, P. Arora, R. Rautela, S. Pant and H. C. Joshi, *J. Lumin.*, 2015, **158**, 412.

30 N. J. Turro, *Modern Molecular Photochemistry*, University Science Books, Sausalito, CA, 1991.

31 T. G. Wormley, *Am. J. Pharmacol.*, 1894, 561, Entitled On Some of the Tests for Quinine, this paper provides an account of the fluorescence properties of quinine in solution on addition of various acids, oxysalts and halides.

32 J. E. O'Reilly, *J. Chem. Educ.*, 1975, **52**, 610.

33 O. S. Wolfbeis and H. Offenbacher, *Monatsh. Chem.*, 1984, **115**, 647.

34 (a) A. N. Swinburne, M. J. Paterson, A. Beeby and J. W. Steed, *Org. Biomol. Chem.*, 2010, **8**, 1010; (b) M. S. Mehata and H. B. Tripathi, *J. Lumin.*, 2002, **99**, 47.

35 R. Badugu, H. Szmacinski, E. A. Reece, B. H. Jeng and J. R. Lakowicz, *Anal. Biochem.*, 2020, **608**, 113905.

36 E. A. Kataev, *Chem. Commun.*, 2023, **59**, 1717.

37 D. C. Magri, *Analyst*, 2015, **140**, 7487.

38 (a) G. J. Scerri, J. C. Spiteri, C. J. Mallia and D. C. Magri, *Chem. Commun.*, 2019, **55**, 4961; (b) D. C. Magri, M. Camilleri Fava and C. J. Mallia, *Chem. Commun.*, 2014,

50, 1009; (*c*) D. C. Magri, G. J. Brown, G. D. McClean and A. P. de Silva, *J. Am. Chem. Soc.*, 2006, **128**, 4950.

39 S. A. de Silva, B. Amorelli, D. C. Isidor, K. C. Loo, K. E. Crooker and Y. E. Pena, *Chem. Commun.*, 2002, 1360.

40 S. A. de Silva, K. C. Loo, B. Amorelli, S. L. Pathirana, M. Nyakirang'ani, M. Dharmasena, S. Demarais, B. Dorcley, P. Pullay and Y. A. Salih, *J. Mater. Chem.*, 2005, **15**, 2791.

41 H. Yokoo, A. Ohsaki, H. Kagechika and T. Hirano, *Tetrahedron*, 2016, **72**, 5872.

42 P. Ceroni, G. Bergamini and V. Balzani, *Angew. Chem., Int. Ed.*, 2009, **48**, 8516.

43 D. Margulies, G. Melman and A. Shanzer, *J. Am. Chem. Soc.*, 2006, **128**, 4865.

44 U. Pischel and J. Andréasson, *New J. Chem.*, 2010, **34**, 2701.